Electronic and vibrational properties of diamondlike hydrocarbons

A. J. Lu,[1] B. C. Pan,[1,*] and J. G. Han[2]
[1]*Hefei National Laboratory for Physical Sciences at Microscale, and Department of Physics, University of Science and Technology of China, Hefei, Anhui 230026, P.R.China*
[2]*Department of Chemistry, Jackson State University, Jackson, Mississippi 39217, USA*
(Received 14 February 2005; published 15 July 2005)

The electronic and vibrational properties of small diamondoids are systematically investigated using an *ab initio* molecular orbital method. The obtained formation energies, ionization potentials, and affinity energies as well as the HOMO-LUMO gaps of the concerned diamondoids all exhibit the polymantane-order-dependent feature. We also propose the fragmentation channels with the lowest dissociation energies of cationic and neutral products, based on our calculated dissociation energies of the neutrals and positively charged diamondoids. It is, furthermore, revealed that the products arising from the dissociation of a diamondoid preferably contain some tiny hydrocarbons. In addition, the vibrational frequencies of the diamondoids are predicted, which may serve as a reference in identifying the hydrocarbon systems in the experiment.

DOI: 10.1103/PhysRevB.72.035447 PACS number(s): 33.15.−e, 31.15.Ar, 63.22.+m

I. INTRODUCTION

Diamondoids are a peculiar class of hydrocarbons, which can be isolated from petroleum or synthesized in laboratories.[1–7] These molecules typically characterize diamond face-fused cages with hydrogen terminated dangling bonds. Such distinctive structures are responsible for outstanding stability, light weight, and rigidity. Therefore, the diamondoid hydrocarbons are promising in many fields. For example, they can be used as seeds for CVD diamond production and templates for crystallization of some crystals; adamantane and derivatives have been applied in chemical industry and polymer synthesis.[8,9] As for an application to the pharmaceutics, adamantane has also been an important composition of related medicines to treat cancer or tumor.[10] More recently, as an indicator of the maturity of natural oil cracking, diamondoid hydrocarbons are used effectively to assess the maturity of natural gas.[2,4] In the oil industry diamondoids are known dissolved in oil and regarded as nucleation sites for the sludge formation, which probably results in the pipeline blockage.[11]

Experimentally, Teja *et al.*[12] studied the solubilities of diamondoids in supercritical solvents. Their experimental results exhibit linear trends between logarithm of the solubility and solvent reduced density. Carlson[7] and other groups[2,3] used gas chromatography-mass spectrometry (GC-MS) to distinguish the different molecules and estimate their relative abundance in crude oils.

On the theoretical side, Tomanek[13] and co-workers predicted a size dependence of the energetic and electronic properties of the diamondoids through local density approximation (LDA) calculation. They pointed out that the energy gap of the diamondoid reduces as the size of a diamondoid molecule increases. This finding is in good agreement with the results from Galli *et al.*[14]

Evidently, although the diamondoids are very important in applied science, there are a few data about their geometrical and electronic structures available from both experiments and theoretical calculations so far. To gain an insight into the diamondoids, we, in this work, employ a high level *ab initio* molecular-orbital theory to calculate the concerned diamondoids. We not only obtain more detailed electronic properties including ionization potentials (IP's) and the affinity energies (AE's) of the diamondoids but predict the vibrational frequencies for each considered diamondoid molecule as well. The possible dissociation path of the diamondoids is discussed in detail too.

II. COMPUTATIONAL DETAILS

We employ Gaussian 98 quantum chemistry software[15] at the B3LYP/6-31G(d) level of density functional theory to calculate the diamondoids. In a benchmark calculation at the chosen B3LYP/6-31G(d) level, the optimized geometry of a CH_4 molecule shows the C-H bond length of 1.094 Å, in excellent agreement with that (1.094 Å) from experiment.[17] The calculated ionization potential of this molecule is 12.85 eV, consistent with the value of 12.99 eV from experiment[16] very well. We also compute the vibrational frequencies of a CH_4 for more tests. The obtained vibrational frequencies are 3051 cm^{-1} (A_1), 1594 cm^{-1} (E), 3161 cm^{-1} (T_2) and 1374 cm^{-1} (T_2), in good agreement with those from experiment[17] and previous calculations.[18] Such a testing calculation indicates that it is reliable and sufficient to handle the diamondoid hydrocarbons we concerned by using the Gaussian 98 package at B3LYP/6-31G(d) level.

III. GEOMETRIES AND ENERGETICS

In this work, twenty eight diamondoids (Fig. 1) reported by Carlson *et al.*[7] are considered. Among them adamantane [Fig. 1(1)] is the smallest diamondoid hydrocarbon, consisting of ten carbon atoms and sixteen hydrogen atoms. Basically, adamantane is of a cage-shaped structure whose carbon skeleton is a basic portion in the carbon diamond. Such a cage-shaped structure can be regarded as a subunit to form other higher polymantane order diamondoids. For example, there are two subunits in a diamantane [Fig. 1(2)], three in a triamantane [Fig. 1(3)], and so on.

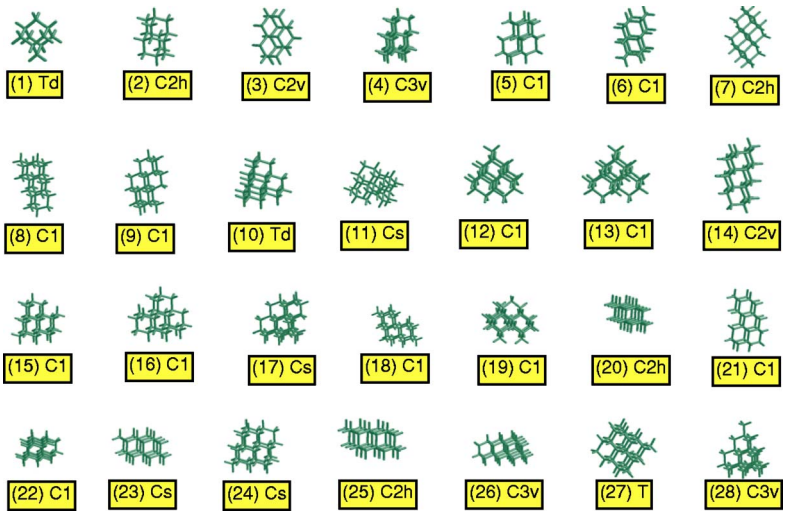

FIG. 1. (Color online) The skeletons of the considered diamondoid molecular structures and their point group symmetries. (1) Adamantane, (2) diamantane, (3) triamantane, (4)–(7) tetramantane, (8)–(16) pentamantane, (17)–(22) hexamantane, (23)–(24) heptamantane, (25) octamantane, (26) nanomantane, (27) decamantane, and (28) alkyl-pentamantane. The atomic structures of these diamondoids are available via bcpan@ustc.edu.cn.

We fully relax these diamondoids, and then systematically analyze the bond lengths and bond angles for the resulting isomers. Our finding is that the averaged bond length of C-C bonds is around 1.545 Å, and the averaged value of C-H bond lengths is about 1.10 Å. The former matches the C-C bond length in bulk diamond very well. As increasing the polymantane size of the diamondoid, the averaged C-C and C-H bond lengths of the diamondoid increase slightly [Figs. 2(a) and 2(b)], whereas the averaged bond angle decreases as the polymantane size of diamondoid increases [Fig. 2(c)]. Overall, the averaged bond angles of most isomers are less than the bond angle (109.47°) of C-C-C in the bulk diamond structure. This is because the C-H bonds existed in the diamondoids make contributions of smaller bond angles of C-C-H or/and H-C-H to the averaged bond angles. Our obtained results above confirm the findings from Tomanek *et al.*[13]

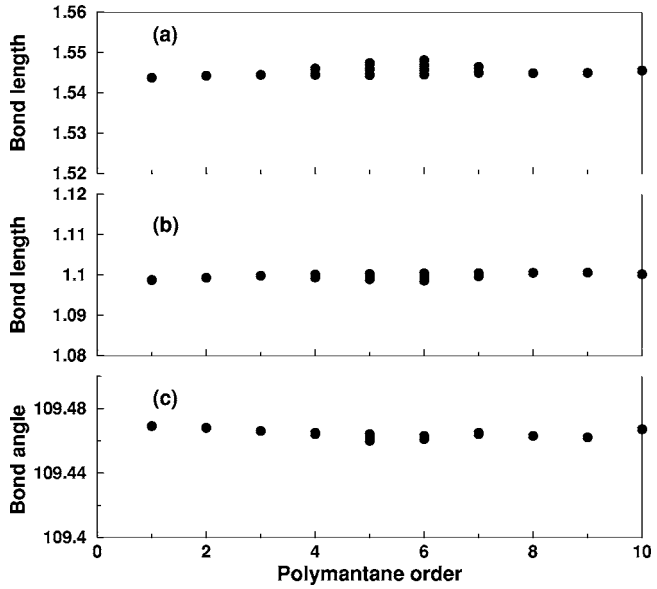

FIG. 2. (a) averaged bond length of C-C bonds in diamondoids versus polymantane order; (b) averaged bond length of C-H bonds in diamondoids versus polymantane order; (c) averaged bond angle of diamondoids versus the polymantane order.

In order to make a comparison of the relative stabilities between the concerned diamondoids, we calculate the cohesive energies per carbon atom for each diamondoid. The cohesive energy per carbon atom of a diamondoid is defined by $\Delta E=[E_{tot}(C_nH_m)-nE_C-mE_H]/n$, where $E_{tot}(C_nH_m)$ is the total energy of the diamondoid molecule, E_C is the energy of a single carbon atom, and E_H the energy of a single hydrogen atom.[19] n and m are the numbers of carbon and hydrogen atoms in a hydrocarbon system, respectively. From our calculated cohesive energy curve (Fig. 3), it is observed that, when the polymantane order of the diamondoid increases from 1 to 10, the cohesive energy of the related diamondoid increases in the whole considered size range, except for the case at polymantane order 5. For this case, an isomer with point group symmetry of C_{3v} [diamondoid(28) in Fig. 1] is more stable than its neighboring polymantane-sized isomers energetically. It seems that the alkyl-pentamantane is probably a magic number cluster in our considered size range of the diamondoids.

IV. IONIZATION POTENTIALS AND ELECTRON AFFINITIES

To evaluate the ionization potentials (IP's) and electron affinities (AE's) of the concerned diamondoids, we calculate

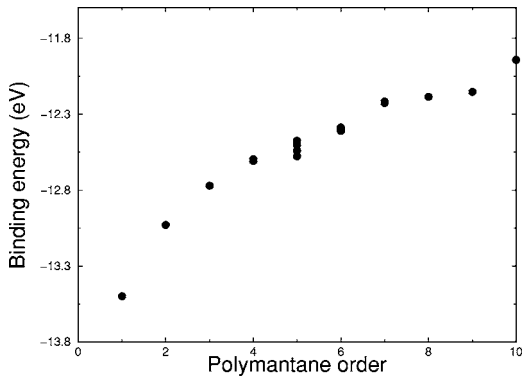

FIG. 3. Binding energies of diamondoid hydrocarbons versus the polymantane order.

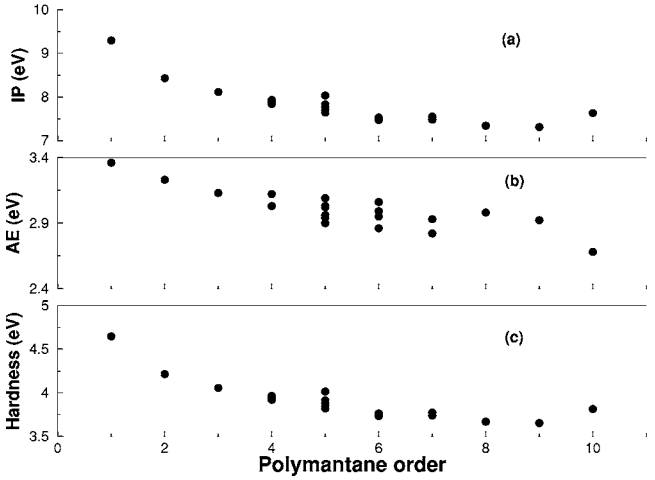

FIG. 4. (a) IP's of diamondoids versus polymantane order. (b) AE's of diamondoids versus polymantane order. (c) The hardness of diamondoids versus the polymantane order.

the total energies of the positively and negatively charged isomers with full relaxations respectively, and then obtain the adiabatic IP (AE) of each isomer by making energy difference between the positively (negatively) charged isomer and the related neutral isomer. Figure 4 plots the calculated IP's and AE's of the diamondoids. From Fig. 4, it is observed that the values of the IP's of the diamondoids vary from 7.5 eV to 9.5 eV, and the AE's range from 3.5 eV to 2.5 eV. Clearly, the IP value is always larger than that of AE for each considered isomer, implying that it is easier to gain an electron to a diamondoid isomer than to remove an electron from the diamondoid isomer. Overall, the obtained IP's and AE's in this work show a size-dependent feature. That is, both IP's and AE's decrease as the size of the low-energy isomer increases. Moreover, the calculated IP's and AE's of each isomer can be used to describe the chemical hardness of the isomer according to the definition of hardness from Parr and Pearson.[20,21] Our calculation clearly indicates that the hardness of diamondoid molecule decreases as the molecular size increases, as shown in Fig. 4(c).

TABLE I. Possible dissociations of the lowest-energy diamondoids at the considered polymantane orders. The numbers listed in the brackets are the polymantane orders of the diamondoids.

Reactant	Products	Energy (eV)
$C_{35}H_{36}(10)$	$C_{30}H_{34}(7)+C_5H_2$	+6.80
$C_{35}H_{36}(10)$	$C_{30}H_{36}(6)+C_5$	+9.87
$C_{38}H_{42}(9)$	$C_{34}H_{38}(8)+C_4H_4$	+3.27
$C_{34}H_{38}(8)$	$C_{30}H_{34}(7)+C_4H_4$	+3.29
$C_{34}H_{38}(8)$	$C_{30}H_{36}(6)+C_4H_2$	+4.77
$C_{30}H_{34}(7)$	$C_{26}H_{32}(5)+C_4H_2$	+4.30
$C_{30}H_{34}(7)$	$C_{27}H_{34}(5)+C_3$	+7.64
$C_{30}H_{36}(6)$	$C_{26}H_{32}(5)+C_4H_4$	+3.05
$C_{30}H_{36}(6)$	$C_{27}H_{34}(5)+C_3H_2$	+5.28
$C_{26}H_{32}(5)$	$C_{22}H_{28}(4)+C_4H_4$	+3.39
$C_{22}H_{28}(4)$	$C_{18}H_{24}(3)+C_4H_4$	+3.28
$C_{18}H_{24}(3)$	$C_{14}H_{20}(2)+C_4H_4$	+3.24
$C_{14}H_{20}(2)$	$C_{10}H_{16}(1)+C_4H_4$	+3.19

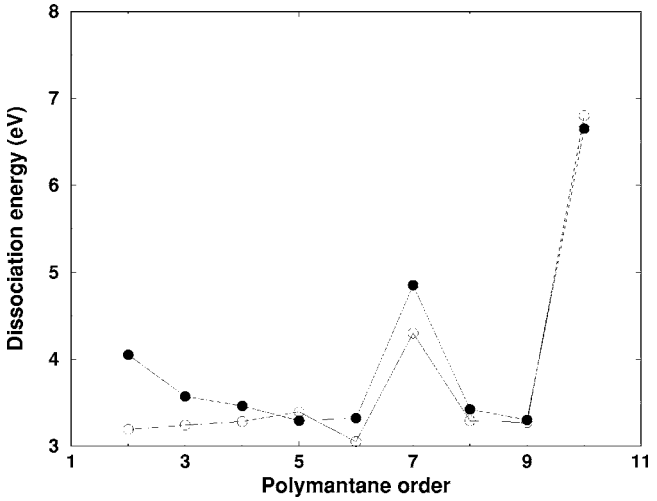

FIG. 5. The lowest dissociation energy curves of the considered cationic (solid circles) and neutral (circles) diamondoids.

V. POSSIBLE DISSOCIATIONS OF THE DIAMONDOIDS

Fragmentation channels with the lowest dissociation energies of cationic and neutral products are of importance for deep understanding of clusters and molecules. Usually, the process of dissociation of a diamondoid is controlled thermodynamically. This implies that the resulting fragments are physically corresponding to the isomers with lowest energy. Thus, the lowest-energy dissociation occurs between the lowest-energy fragments. Commonly, the dissociation energy of a diamondoid along the channel leading to two smaller fragments is defined as

$$D(n_1,n_2;m_1,m_2) = (E_{n_1,m_1} + E_{n_2,m_2}) - E_{n_1+n_2,m_1+m_2}, \quad (1)$$

where $E_{n_1+n_2,m_1+m_2}$ is the total energy of a diamondoid consisting of (n_1+n_2) carbon atoms and (m_1+m_2) hydrogen at-

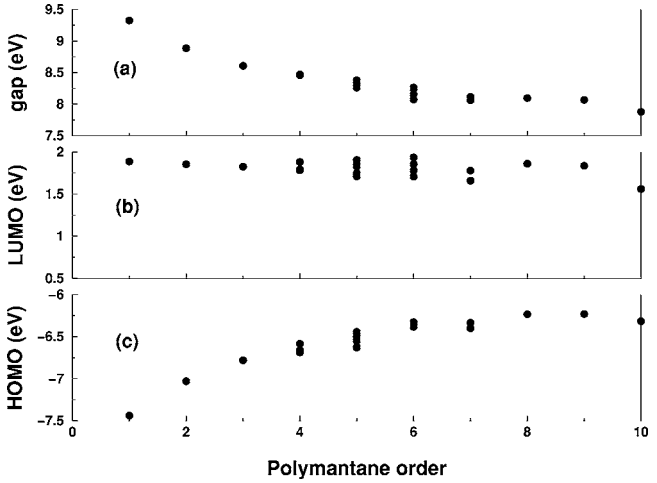

FIG. 6. The HOMO-LUMO gaps (a), the HOMO energy levels (b), and the LUMO energy levels (c), as a function of the polymantane order.

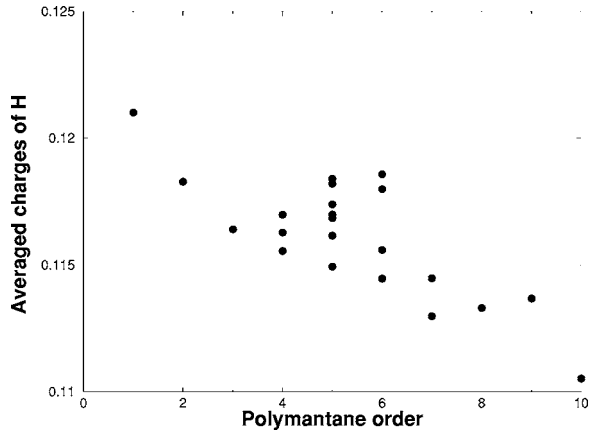

FIG. 7. The averaged values of lost electrons in hydrogen atoms versus the polymantane order.

oms, E_{n_1,m_1} the total energy of a resulting fragment consisting of n_1 carbon atoms and m_1 hydrogen atoms, and E_{n_2,m_2} the total energy of the other produced fragment consisting of n_2 carbon atoms and m_2 hydrogen atoms. At first, we examine whether a diamondoid with high polymantane order can be dissociated into two diamondoids with lower polymantane order without any other product. Our answer is negative yet. So, we restrict our attention to the possible dissociation from a considered lowest-energy diamondoid with high polymantane order to a considered lowest-energy diamondoid with lower polymantane order plus a product with very smaller size, such as C_4H_4, C_5H_2, C_4H_2, C_3H_2, C_5, or C_3. Our calculations show that the loss of C_4H_4 occurs for the most dissociations between the neighboring diamondoids as listed in Table I. In order to evaluate the lowest-energy dissociation path, we calculate the energies of ground-state structures of C_4H_4, C_5H_2, C_4H_2, C_3H_2, C_5, and C_3, respectively. Inserting the calculated total energies of related diamondoids and the by-product into Eq. (1), we immediately obtain the dissociation energies of the diamondoids, which are also listed in Table I. The findings from Table I are that, although the isomer $C_{27}H_{34}$ at polymantane order 5 is probably a magic cluster as mentioned above, this isomer is energetically unfavorable to be formed from the dissociation of the lowest-energy isomer at polymantane order of either 6 or 7. Instead,

TABLE II. Vibrational frequencies (cm^{-1}) and the IR-active intensities in the brackets of diamondoid(1) with polymantane order 1.

A_1	756.87, 1061.91, 1551.05, 3020.89, 3054.74
A_2	1141.43
E	416.40, 922.83, 1250.64, 1423.25, 1515.02, 3025.65
T_1	342.15, 912.83, 1061.61, 1141.69, 1330.43, 1368.77, 3061.06
T_2	459.75(0.1), 817.64(0.1), 986.85(0.9), 1130.40(2.9), 1355.51(0.3), 1409.45(0.8), 1528.66(7.2), 3023.83(13.9), 3042.56(159.4), 3066.73(94.4)

TABLE III. Vibrational frequencies (cm^{-1}) and the IR-active intensities in the brackets of diamon- doid(2) with polymantane order 2.

A_g	409.65, 430.70, 458.02, 646.16, 708.94, 806.52, 893.05, 947.50, 991.98, 1045.82, 1085.76, 1109.22, 1209.21, 1269.56, 1344.20, 1371.41, 1378.53, 1399.22, 1432.60, 1515.50, 1532.91, 3010.51, 3015.68, 3024.83, 3033.92, 3051.56, 3062.72
A_u	269.53(0.0), 297.48(0.0), 397.96(0.1), 620.04(0.0), 808.58(0.1), 875.73(0.0), 938.37(0.0), 1062.47(0.1), 1067.96(4.1), 1082.70(2.0), 1148.13(0.0), 1179.70(0.1), 1297.27(0.0), 1320.45(0.5), 1363.49(0.2), 1389.08(0.2), 1428.18(0.1), 1512.63(7.1), 3014.61(6.0), 3031.24(210.3), 3056.73(1.9), 3062.51(150.0)
B_g	336.04, 410.97, 433.16, 646.71, 895.23, 916.61, 949.94, 1046.07, 1110.13, 1161.67, 1210.15, 1269.27, 1346.41, 1365.13, 1369.30, 1399.68, 1512.34, 3012.26, 3025.16, 3056.93, 3061.66
B_u	298.23(0.0), 396.64(0.1), 619.93(0.0), 697.22(0.9), 804.61(0.1), 808.33(0.5), 936.07(0.04), 991.09(0.3), 1067.55(4.7), 1079.54(1.6), 1099.29(1.0), 1179.06(0.1), 1291.27(0.0), 1320.60(0.5), 1364.86(0.2), 1388.94(0.2), 1398.76(4.8), 1427.02(0.1), 1515.90(7.2), 1535.25(9.1), 3009.22(48.9), 3014.07(9.9), 3023.41(6.9) , 3030.26(208.4), 3046.24(235.3), 3063.60(150.2)

the lowest-energy isomers at polymantane order of both 6 and 7 are favorably dissociated into a $C_{26}H_{32}$ [diamondoid(10)] plus a smaller hydrocarbon C_4H_2. Thus, at polymantane order of 5 the existence of the metastable isomer of $C_{26}H_{32}$ [diamondoid(10)] is not ignorable, even though the energetic stability of this isomer is slightly less than the magic cluster ($C_{27}H_{34}$). This situation is actually due to that the total energy of a C_4H_2 is lower than that of a C_3, so that the resulted $C_{26}H_{32}+C_4H_2$ is more stable than $C_{27}H_{34}+C_3$. In general, hydrogenation of a tiny carbon cluster can remove parts or all of the dangling bonds in the tiny carbon cluster, enhancing the energetic stability of the tiny carbon cluster. As a consequence, the lowest-energy dissociations of the diamondoids we considered above yield almost fragments containing a tiny hydrocarbon molecule not a tiny carbon cluster. This is probably valid for a lowest-energy dissociation of *any* large sized diamondoid and hydrocarbon molecule. On the other hand, the lowest dissociation energy pathway obtained from our calculations does exhibit two local maxima at polymantane orders of both 5 and 7 (as plotted in Fig. 5). Such aspects reflect that, as compared to the diamondoids at the other polymantane orders, the isomers at the polymantane orders of 5 and 7 become more abundant in the considered diamondoids.

Similarly, we also evaluate the dissociation energies of positively charged diamondoids. Our calculations show that a positively charged diamondoid is preferably dissociated into a positively charged diamondoid with lower polyman-

TABLE IV. Vibrational frequencies (cm^{-1}) and the IR-active intensities in the brackets of diamon- doid(3) with polymantane order 3.

A_1	314.81(0.1), 405.40(0.1), 500.24(0.0), 566.74(0.1), 662.63(0.0), 760.46(0.3), 835.51(0.0), 869.20(0.0), 962.56(0.5), 1002.46(0.6), 1024.08(2.1), 1086.90(1.3), 1146.86(3.5), 1212.29(0.3), 1298.60(0.4), 1328.91(1.4), 1363.50(2.5), 1386.69(0.0), 1401.60(0.5), 1414.73(0.0), 1511.79(7.6), 1530.85(1.7), 2977.02(20.1), 2993.38(0.1), 3014.96(49.4), 3016.97(70.3), 3029.27(193.9), 3046.48(4.6), 3054.21(173.4)
A_2	246.56, 365.20, 449.23, 589.17, 904.56, 939.26, 1055.33, 1072.00, 1105.84, 1169.53, 1193.42, 1253.23, 1330.21, 1357.24, 1389.62, 1505.92, 3007.74, 3041.80, 3057.74
E	227.70(0.0), 315.40(0.0), 363.63(0.0), 392.90(0.0), 423.72(0.2), 441.36(0.0), 486.90(0.1), 570.44(0.1), 688.00(0.7), 770.80(0.4), 813.92(0.8), 865.17(0.0), 890.27(0.1), 903.76(0.0), 955.54(0.5), 966.83(0.0), 1011.09(0.0), 1037.16(0.0), 1063.99(0.1), 1078.03(0.0), 1089.44(0.1), 1135.73(1.5), 1179.77(0.0), 1190.06(0.3), 1202.46(0.7), 1243.37(0.1), 1287.41(0.0), 1318.07(0.1), 1341.68(0.0), 1347.69(0.1), 1358.98(1.6), 1384.93(0.0), 1388.83(0.0), 1398.03(1.1), 1406.47(1.1), 1421.67(0.0), 1508.19(2.7), 1513.52(0.8), 1527.11(6.8), 2992.30(29.3), 3007.33(3.7), 3009.03(4.3), 3014.37(65.8), 3023.91(21.4), 3049.15(16.3), 3043.13(191.6), 3043.95(3.3), 3059.32(98.3)

TABLE V. Vibrational frequencies (cm^{-1}) and the IR-active intensities in the brackets of diamondoid(4) with polymantane order 4.

A_1	338.32(0.3), 396.14(0.2), 445.83(0.0), 507.15(0.0), 569.60(0.1), 640.45(0.0), 762.96(0.7), 799.90(0.1), 860.22(0.0), 868.72(0.0), 946.66(0.5), 987.13(0.0), 1010.07(0.0), 1071.04(0.0), 1115.27(0.5), 1167.82(3.2), 1225.83(0.3), 1255.13(0.4), 1310.41(0.7), 1340.37(0.0), 1391.72(3.3), 1396.88(0.0), 1397.14(0.1), 1403.77(0.6), 1408.77(0.1), 1431.66(1.9), 1507.74(4.1), 1522.99(6.4), 1530.65(1.1), 2975.91(15.1), 2980.86(9.1), 3007.80(1.1), 3014.71(155.6), 3018.99(0.5), 3031.88(89.6), 3044.54(31.8), 3054.92(174.8)
A_2	225.36, 245.26, 253.77, 376.87, 472.29, 587.45, 900.79, 903.88, 941.66, 1058.56, 1070.60, 1116.22, 1169.33, 1192.73, 1248.35, 1316.30, 1345.48, 1387.41, 1506.09, 3008.51, 3034.86, 3042.05, 3049.52
E	209.17(0.0), 246.70(0.0), 301.81(0.0), 346.19(0.2), 382.68(0.0), 391.31(0.0), 427.92(0.1), 473.00(0.0), 483.95(0.0), 485.35(0.0), 576.20(0.1), 608.29(0.0), 776.73(1.0), 826.64(1.0), 856.21(0.0), 864.80(0.3), 901.03(0.0), 927.91(0.0), 958.51(0.0), 976.96(0.0), 997.62(0.1), 1034.01(0.0), 1047.18(0.0), 1065.02(0.0), 1088.98(0.0), 1101.32(0.0), 1112.79(0.0), 1136.90(0.7), 1180.76(1.5), 1210.48(0.6), 1215.73(0.7), 1242.90(0.0), 1298.27(0.7), 1314.09(0.1), 1324.93(0.0), 1336.11(0.0), 1345.95(0.0), 1349.81(0.0), 1386.33(0.9), 1389.11(0.1), 1394.09(0.0), 1402.74(0.8), 1501.45(0.0), 1508.35(3.2), 1513.06(0.7), 1524.64(1.7), 1526.60(9.4), 2973.37(23.8), 3001.44(20.2), 3009.49(12.5), 3012.79(3.4), 3015.29(99.1), 3040.57(10.3), 3041.95(181.5), 3044.35(0.1), 3048.54(5.3), 3053.64(129.8), 3097.14(36.6)

tane order and a tiny neutral hydrocarbon, where the produced tiny neutral hydrocarbon is the same as that from the dissociation of the related neutral diamondoid as listed in Table I. The lowest dissociation energy curve of the positively charged diamondoids is also displayed in Fig. 5. The finding from Fig. 5 is that the lowest dissociation energies of the positively charged diamondoids are comparable to those of the neutral diamondoids at each polymantane order. Typi-

TABLE VI. Vibrational frequencies (cm^{-1}) and the IR-active intensities in the brackets of diamondoid(28) with polymantane order 5.

A_1	338.32(0.3), 396.14(0.2), 445.83(0.0), 507.15(0.0), 569.60(0.1), 640.45(0.0), 762.96(0.7), 799.90(0.1), 860.22(0.0), 868.72(0.0), 946.66(0.5), 987.13(0.0), 1010.07(0.0), 1071.04(0.0), 1115.27(0.5), 1167.82(3.2), 1225.83(0.3), 1255.13(0.4), 1310.41(0.7), 1340.37(0.0), 1391.72(3.3), 1396.88(0.0), 1397.14(0.1), 1403.77(0.6), 1408.77(0.1), 1431.66(1.9), 1507.74(4.1), 1522.99(6.4), 1530.65(1.1), 2975.91(15.1), 2980.86(9.1), 3007.80(1.1), 3014.71(155.6), 3018.99(0.5), 3031.88(89.6), 3044.54(31.8), 3054.92(174.8)
A_2	225.36, 245.26, 253.77, 376.87, 472.29, 587.45, 900.79, 903.88, 941.66, 1058.56, 1070.60, 1116.22, 1169.33, 1192.73, 1248.35, 1316.30, 1345.48, 1387.41, 1506.09, 3008.51, 3034.86, 3042.05, 3049.52
E	209.17(0.0), 246.70(0.0), 301.81(0.0), 346.19(0.2), 382.68(0.0), 391.31(0.0), 427.92(0.1), 473.00(0.0), 483.95(0.0), 485.35(0.0), 576.20(0.1), 608.29(0.0), 776.73(1.0), 826.64(1.0), 856.21(0.0), 864.80(0.3), 901.03(0.0), 927.91(0.0), 958.51(0.0), 976.96(0.0), 997.62(0.1), 1034.01(0.01), 1047.18(0.0), 1065.02(0.0), 1088.98(0.0), 1101.32(0.0), 1112.79(0.0), 1136.90(0.7), 1180.76(1.5), 1210.48(0.6), 1215.73(0.7), 1242.90(0.0), 1298.27(0.7), 1314.09(0.1), 1324.93(0.0), 1336.11(0.0), 1345.95(0.0), 1349.81(0.0), 1386.33(0.9), 1389.11(0.1), 1394.09(0.0), 1402.74(0.8), 1501.45(0.0), 1508.35(3.2), 1513.06(0.7), 1524.64(1.7), 1526.60(9.4), 2973.37(23.8), 3001.44(20.2), 3009.49(12.5), 3012.79(3.4), 3015.29(99.1), 3040.57(10.3), 3041.95(181.5), 3044.35(0.1), 3048.54(5.3), 3053.64(129.8), 3097.14(36.6)

TABLE VII. Vibrational frequencies (cm^{-1}) and the IR-active intensities in the brackets of diamondoid(20) with polymantane order 6.

A_u	135.09(0.0), 150.86(0.0), 293.29(0.0) 365.43(0.1), 375.65(0.1), 386.01(0.0), 426.44(0.1), 490.38(0.0), 646.79(0.0), 715.70(0.0), 810.92(0.0), 862.57(0.1), 899.76(0.1), 906.17(0.0), 947.81(0.0), 997.10(0.3), 1047.04(0.0), 1062.59(0.1), 1073.83(0.2), 1086.74(6.8), 1107.87(1.7), 1138.43(0.3), 1169.16(0.0), 1183.22(0.1), 1210.29(1.2), 1266.64(0.0), 1291.28(0.9), 1314.16(0.1), 1327.37(4.5), 1348.98(0.1), 1360.59(0.1), 1369.39(0.0), 1374.89(0.1), 1393.92(0.2), 1417.17(0.0), 1513.66(6.8), 2987.51(0.5), 3000.32(88.0), 3012.18(65.9), 3026.07(231.4), 3035.73(12.0), 3047.10(21.2), 3049.70(147.0), 3057.56(124.4)
B_u	189.09(0.0), 383.72(0.0), 418.86(0.2), 435.59(0.0), 511.21(0.0), 588.65(0.0), 628.86(0.9), 654.57(0.7), 685.56(0.9), 690.78(0.2), 773.61(0.1), 822.48(0.3), 895.81(0.1), 908.85(0.5), 953.63(1.2), 962.92(0.1), 993.77(0.7), 1039.29(0.5), 1053.18(2.1), 1066.91(1.8), 1089.62(1.4), 1109.16(3.6), 1155.29(1.3), 1170.71(0.9), 1198.96(0.1), 1217.44(0.4), 1274.95(0.7), 1281.10(0.2), 1311.95(0.1), 1338.25(2.7), 1354.82(1.8), 1359.67(0.7), 1383.55(5.4), 1388.61(3.6), 1393.18(1.4), 1414.69(0.8), 1423.10(1.2), 1433.84(0.0), 1510.23(1.4), 1516.18(1.8), 1523.75(13.1), 1533.79(11.9), 2987.86(29.2), 2994.39(13.6), 3002.30(39.0), 3009.17(67.0), 3010.24(23.3), 3015.13(122.5), 3019.82(92.4), 3030.68(194.6), 3046.51(295.9), 3060.39(153.9)
B_g	234.08, 265.58, 355.06, 381.48, 404.30, 413.55, 451.48, 646.42, 650.03, 676.96, 824.32, 898.68, 907.84, 911.64, 941.55, 993.17, 1058.95, 1070.87, 1082.69, 1086.67, 1145.65, 1169.46, 1190.06, 1222.04, 1260.89, 1287.75, 1311.85, 1325.49, 1347.01, 1360.09, 1366.96, 1381.99, 1401.44, 1411.33, 1513.65, 2987.84, 2992.83, 3011.48, 3025.77, 3035.60, 3047.06, 3049.09, 3057.33
A_g	283.26, 323.03, 407.67, 416.77, 421.09, 478.30, 626.06, 643.71, 680.96, 703.25, 726.83, 809.90, 829.68, 898.65, 939.95, 966.29, 972.88, 1038.29, 1053.77, 1065.03, 1070.68, 1099.83, 1132.29, 1146.60, 1165.02, 1193.81, 1211.06, 1273.53, 1291.98, 1313.73, 1341.46, 1349.23, 1365.56, 1375.04, 1389.84, 1395.91, 1399.22, 1426.60, 1433.10, 1510.65, 1516.01, 1521.57, 1533.30, 2988.55 , 2998.00, 3004.59, 3010.02, 3010.97, 3016.13, 3020.34, 3031.95, 3047.41, 3060.35

cally, there is no significant difference between the dissociation energy curves in the polymantane-order range from 6 to 10. However, the basic trends of the two curves ranging from polymantane order 5 to 2 are different: with decreasing the polymantane order of the diamondoid, the lowest dissociation energy of the neutral diamondoid decreases, while the lowest dissociation energy of the positively charged diamondoid increases.

Actually, the dissociation energies of the cations above correlate to the mass spectrum. Unfortunately, there is no experimental mass spectrum of diamondoids available to date. We anticipate that our predicted aspects in the lowest dissociation energy curve of the positively charged diamondoids can be verified in the future.

VI. ELECTRONIC PROPERTY

Previously, Tomanek and co-workers predicted that the energy gap of a diamondoid hydrocarbon not only is larger than 6 eV but also reduces with increasing the size of the diamondoid.[13] Such an aspect is also supported by our calculations [Fig. 6(a)]. Furthermore, our calculations reveal

TABLE VIII. Vibrational frequencies (cm^{-1}) and the IR-active intensities in the brackets of diamondoid(23) with polymantane order 7.

A'	188.24(0.0), 293.01(0.1), 321.65(0.1), 338.40(0.0), 365.14(0.1), 386.49(0.0), 398.70(0.1), 401.02(0.0), 418.12(0.0), 438.20(0.1), 485.26(0.0), 511.92(0.0), 523.73(0.1), 559.33(0.1), 625.24(0.4), 652.14(0.0), 655.54(0.0), 673.33(0.2), 682.73(0.0), 709.85(0.1), 778.97(1.3), 798.45(0.1), 823.05(0.1), 829.11(0.0), 864.18(0.0), 879.64(0.1), 884.39(0.1), 903.88(0.5), 922.26(0.4), 937.57(0.1), 948.76(0.0), 960.35(0.1), 980.78(0.8), 984.93(0.1), 1011.92(0.5), 1029.96(0.3), 1038.72(0.0), 1050.59(0.4), 1062.75(0.1), 1070.70(0.4), 1074.32(0.1), 1082.68(4.5), 1087.10(1.9), 1110.22(0.2), 1129.52(0.0), 1131.34(3.8), 1165.06(0.1), 1173.86(0.1), 1190.82(0.1), 1205.68(0.5), 1215.17(0.7), 1224.14(0.1), 1240.45(0.2), 1261.23(0.0), 1277.48(0.1), 1295.21(0.3), 1305.91(0.2), 1321.55(0.5), 1324.45(0.0), 1343.87(0.0), 1345.12(0.1), 1349.50(3.7), 1358.13(0.9), 1366.82(0.3), 1372.37(0.0), 1380.96(1.4), 1387.75(2.6), 1392.35(0.8), 1399.52(1.0), 1400.35(0.2), 1404.96(0.2), 1406.84(2.0), 1416.42(0.0), 1424.77(0.0), 1425.99(0.0), 1512.57(1.2), 1518.11(4.9), 1518.64(2.0), 1521.14(5.3), 1531.69(5.2), 2972.57(12.4), 2986.92(7.1), 2992.25(11.6), 2994.32(87.8), 2997.32(10.5), 3005.25(32.9), 3008.79(1.9), 3010.48(9.0), 3012.26(54.0), 3014.09(25.8), 3016.03(16.0), 3022.78(188.5), 3025.69(3.5), 3027.78(162.1), 3038.28(182.0), 3044.42(9.4), 3044.87(102.4), 3053.24(95.0), 3055.79(32.9), 3056.39(112.6)
A''	210.04(0.0), 267.19(0.0), 284.60(0.1), 340.55(0.0), 370.62(0.0), 379.53(0.0), 394.13(0.0), 415.00(0.0), 425.07(0.0), 443.94(0.0), 467.92(0.0), 496.28(0.0), 532.51(0.0), 572.19(0.2), 635.55(0.1), 674.65(0.5), 711.49(0.0), 763.15(0.1), 796.87(1.5), 825.96(0.0), 867.47(0.1), 876.90(0.1), 903.70(0.0), 913.71(0.1), 937.51(0.6), 940.92(0.1), 964.77(0.6), 985.32(0.1), 1023.29(0.0), 1031.06(0.2), 1037.96(0.4), 1042.79(0.1), 1061.70(0.1), 1072.79(0.7), 1076.36(0.1), 1078.83(0.0), 1087.22(0.1), 1099.78(0.0), 1118.15(0.2), 1129.22(1.9), 1150.02(0.1), 1176.57(0.0), 1182.80(0.0), 1183.55(0.0), 1193.71(0.2), 1204.85(0.0), 1211.97(0.0), 1223.18(0.2), 1251.05(0.0), 1261.89(0.0), 1286.08(0.1), 1299.99(0.3), 1315.94(0.0), 1322.83(0.0), 1332.77(0.0), 1336.25(0.3), 1339.91(0.0), 1357.76(0.2), 1360.54(0.1), 1366.10(0.0), 1371.33(0.0), 1381.21(0.1), 1382.84(0.7), 1392.49(1.3), 1395.50(0.6), 1402.44(0.5), 1408.75(0.7), 1421.99(0.0), 1425.63(0.0), 1510.21(0.3), 1520.47(9.6), 1521.40(0.1), 2984.52(8.3), 2987.61(5.7), 2994.21(15.7), 3004.86(3.6), 3007.56(5.9), 3009.92(14.3), 3013.06(12.2), 3017.46(3.9), 3020.63(77.8), 3031.39(303.8), 3043.20(2.1), 3048.84(30.6), 3055.61(31.6), 3059.09(67.4)

TABLE IX. Vibrational frequencies (cm^{-1}) and the IR-active intensities in the brackets of diamondoid(25) with polymantane order 8.

A_u	195.77(0.0), 232.88(0.0), 297.71(0.0), 390.48(0.1), 420.91(0.0), 445.30(0.0), 462.71(0.0), 523.06(0.0), 566.75(0.3), 674.76(0.6), 715.48(0.0), 803.08(1.2), 850.99(0.3), 903.21(0.0), 921.20(0.1), 940.03(1.1), 1008.79(0.2), 1040.23(1.4), 1051.88(0.1), 1060.78(0.2), 1067.01(0.0), 1098.06(0.1), 1121.63(1.2), 1138.10(2.3), 1171.83(0.4), 1183.44(0.0), 1202.93(0.8), 1213.66(0.4), 1252.09(0.0), 1297.53(0.2), 1311.95(0.1), 1335.14(0.2), 1341.38(0.5), 1354.61(1.0), 1368.14(0.0), 1382.11(0.1), 1394.30(0.5), 1407.56(1.6), 1424.45(0.0), 1510.31(0.7), 1520.28(11.5), 2986.12(22.8), 2995.03(30.5), 3005.93(0.9), 3012.64(48.6), 3026.29(362.9), 3043.47(2.2), 3048.88(59.2), 3059.39(131.7)
B_u	156.13(0.0), 297.43(0.1), 387.29(0.0), 391.76(0.0), 408.46(0.0), 463.73(0.2), 493.86(0.0), 537.14(0.0), 567.90(0.0), 669.39(0.7), 713.59(0.5), 782.65(1.5), 810.40(0.1), 839.97(1.5), 872.97(0.0), 895.68(0.1), 930.85(0.4), 960.80(0.7), 1000.62(0.2), 1029.09(0.4), 1038.53(0.0), 1051.29(1.4), 1069.87(1.2), 1094.13(2.0), 1129.38(5.9), 1134.05(0.8), 1186.16(0.0), 1196.80(0.6), 1219.08(3.3), 1255.67(0.8), 1273.25(1.1), 1304.62(0.9), 1324.62(0.2), 1334.05(3.1), 1350.91(4.3), 1367.55(1.3), 1370.30(0.1), 1390.07(1.3), 1392.45(5.6), 1398.14(0.3), 1406.29(0.9), 1417.82(0.5), 1512.27(2.9), 1518.95(7.9), 1531.31(11.0), 2974.00(24.7), 2990.71(37.7), 2994.83(57.3), 3007.36(74.2), 3012.00(39.9), 3014.32(48.7), 3018.29(192.3), 3026.63(176.0), 3044.28(289.5), 3044.92(35.8), 3053.52(234.6)
A_g	286.39, 308.52, 347.56, 401.77, 428.11, 485.59, 533.17, 599.26, 656.17, 676.79, 703.91, 736.81, 807.87, 831.52, 864.22, 903.19, 923.64, 955.19, 977.80, 998.96, 1032.44, 1061.06, 1071.27, 1075.96, 1113.09, 1141.51, 1160.66, 1181.26, 1216.31, 1226.66, 1259.63, 1286.88, 1308.26, 1327.57, 1341.54, 1359.96, 1376.31, 1383.73, 1391.87, 1401.30, 1406.96, 1425.87, 1427.66, 1512.62, 1518.00, 1531.42, 2973.98, 2991.70, 2997.04, 3006.39, 3012.50, 3014.64, 3025.20, 3030.43, 3044.73, 3045.23, 3053.07
B_g	249.30, 332.88, 358.57, 382.97, 408.67, 433.33, 477.01, 534.89, 602.32, 719.11, 779.55, 879.83, 903.69, 915.53, 952.92, 972.43, 1024.98, 1036.68, 1061.19, 1084.23, 1099.00, 1114.08, 1128.37, 1183.36, 1192.00, 1204.56, 1241.71, 1280.42, 1283.32, 1320.04, 1326.79, 1339.49, 1357.90, 1369.31, 1382.11, 1394.11, 1397.72, 1421.36, 1510.25, 1521.11, 2985.26, 2994.40, 3007.06, 3012.48, 3016.56, 3043.52, 3048.88, 3059.27

that, with increasing the polymantane size of the molecule, the energy levels of the lowest unoccupied molecular orbitals (LUMO's) vary slightly but the energy levels of the highest occupied molecular orbitals (HOMO's) show a steady increasing, as displayed in Figs. 6(b) and 6(c). As a consequence, the HOMO-LUMO gap becomes narrow when the polymantane order of the diamondoid hydrocarbon increases. Thus the evolution of HOMO-LUMO gaps of the various diamondoids is mainly originated from the different energy shifts of the HOMO's.

We also calculate the Mulliken charges for the considered isomers. It is observed that all of the H atoms in each hydrocarbon molecule lose their electron charges partly, and the carbon atoms bonding to the H atoms gain electrons. Such transfer of electron charges is very weak due to the values of electronegativity of H and C are close to each other. It is more interesting to note that the values of the lost electron charges in H atoms are somewhat dependent upon the size and shape of the diamondoid molecule, as shown in Fig. 7. Combining the results in Fig. 7 with that in Fig. 3, we can find that the trend of the formation energies of the various diamondoids just correlates to the lost electron charges in the H atoms. Moreover, the more the lost electron charges of the H atoms in a diamondoid are, the more stable the diamon-

TABLE X. Vibrational frequencies (cm^{-1}) and the IR-active intensities in the brackets of diamondoid(26) with polymantane order 9.

A_1	208.97(0.0), 327.25(0.1), 367.70(0.0), 403.37(0.0), 452.67(0.1), 508.46(0.1), 615.67(0.0), 635.00(0.0), 662.52(0.0), 717.08(0.1), 798.02(0.1), 838.87(0.1), 872.44(0.0), 902.99(0.1), 956.08(0.0), 964.61(0.2), 1015.34(0.3), 1057.55(3.3), 1070.69(3.3), 1094.19(0.2), 1148.05(0.1), 1176.52(4.1), 1202.80(0.1), 1241.48(0.3), 1291.01(0.4), 1309.13(1.6), 1348.69(0.1), 1364.20(5.5), 1370.10(0.7), 1390.07(0.3), 1399.42(0.1), 1412.25(0.0), 1430.89(0.0), 1506.86(0.2), 1515.49(9.4), 1531.02(1.8), 2980.73(61.9), 2991.30(5.9), 2997.98(48.8), 3003.66(5.2), 3014.50(159.4), 3017.59(57.1), 3028.02(206.1), 3035.96(14.3), 3045.61(9.1), 3053.51(212.4)
A_2	218.61, 358.02, 390.01, 422.82, 444.20, 575.73, 650.87, 796.26, 898.22, 925.51, 974.48, 1046.29, 1054.72, 1065.15, 1113.57, 1118.43, 1178.24, 1195.16, 1211.99, 1290.69, 1313.53, 1334.51, 1344.39, 1352.55, 1364.80, 1389.31, 1422.56, 1509.94, 2990.19, 3011.98, 3046.15, 3058.85
E	174.50(0.0), 241.08(0.1), 277.03(0.0), 316.90(0.1), 358.25(0.03), 399.19(0.0), 416.47(0.1), 429.54(0.1), 440.59(0.1), 465.30(0.0), 506.21(0.01), 587.04(0.0), 622.06(0.6), 644.68(1.1), 679.27(0.0), 705.01(0.0), 725.67(0.01), 815.76(0.0), 830.77(0.1), 862.12(0.0), 889.49(0.0), 902.30(0.2), 906.18(0.80), 937.19(0.0), 953.72(0.1), 976.24(0.0), 996.43(0.5), 1021.25(0.0), 1040.93(0.5), 1059.37(0.0), 1072.50(0.0), 1078.67(0.2), 1083.45(0.1), 1097.82(0.0), 1110.52(0.2), 1127.90(0.1), 1136.55(2.9), 1153.43(0.0), 1183.51(0.1), 1195.45(0.0), 1205.50(0.1), 1221.14(0.0), 1245.99(0.0), 1250.00(0.1), 1277.35(0.0), 1300.03(0.2), 1312.93(0.1), 1323.07(0.0), 1333.50(0.6), 1335.62(0.1), 1351.29(0.0), 1360.32(2.0), 1370.57(0.0), 1385.23(0.1), 1389.29(1.4), 1392.49(1.1), 1396.61(0.1), 1403.95(1.7), 1413.15(0.1), 1421.70(0.1), 1504.81(0.1), 1512.11(2.3), 1517.29(3.7), 1529.54(7.1), 2971.14(0.1), 2983.64(10.9), 2990.46(1.0), 2997.24(13.2), 3002.58(47.1), 3012.15(5.7), 3013.02(35.1), 3015.26(99.2), 3025.95(25.1), 3035.33(5.8), 3044.21(231.2), 3047.27(10.7), 3051.38(24.8), 3059.35(97.0)

TABLE XI. Vibrational frequencies (cm^{-1}) and the IR-active intensities in the brackets of diamondoid(27) with polymantane order 10.

A	445.24, 509.50, 657.18, 773.88, 984.53, 1061.76, 1062.32, 1196.99, 1239.11, 1243.18, 1381.77, 1406.09, 1416.80, 1525.94, 3005.01, 3017.02, 3040.87
E	402.94, 348.46, 657.59, 858.76, 902.79, 994.97, 1087.07, 1170.09, 1215.82, 1292.84, 1348.07, 1415.56, 1419.50, 1526.48, 2997.99, 3010.00, 3030.93
T	283.89(0.0), 349.31(0.2), 421.33(0.0), 423.92(0.1), 470.73(0.1), 501.06(0.0), 526.71(0.0), 545.98(0.4), 567.21(0.0), 755.12(0.0), 780.59(0.3), 818.43(2.5), 894.97(0.1), 895.89(0.0), 932.38(1.5), 955.19(0.0), 967.08(0.0), 1033.50(0.3), 1063.36(0.2), 1066.91(0.0), 1079.20(0.0), 1088.78(0.0), 1093.97(2.2), 1112.80(0.0), 1132.30(0.0), 1199.38(1.2), 1200.34(0.0), 1216.48(0.7), 1218.36(0.0), 1276.50(0.1), 1277.94(0.0), 1313.55(0.0), 1345.84(0.0), 1357.40(0.0), 1361.26(0.0), 1368.29(0.0), 1380.85(0.1), 1394.30(2.0), 1401.75(0.0), 1415.90(0.0), 1416.92(3.0), 1426.84(0.7), 1526.27(6.8), 2997.91(0.0), 2998.47(13.7), 3004.57(97.3), 3011.69(10.2), 3015.01(0.0), 3022.18(49.3), 3033.72(404.1), 3059.80(0.0), 3060.88(84.1)

doid is. This can be understood as below: without termination of the H atoms, the carbon atoms at the surface of the bare carbon isomers give rise to the dangling bond states lying within the HOMO-LUMO gaps. The H atoms terminating on these dangling bond atoms can effectively remove the dangling bond states from the gaps. That is, the antibonding states of the gap states rise up into the conductive bands, and the bonding states sink down into the valence bands. Thus the passivation of the dangling bonds results in more electron charges transferred between the H atoms and the C atoms. This not only increases the width of the HOMO-LUMO gap but also lowers the energy of the system, enhancing the stability of the system energetically.

VII. VIBRATIONAL FREQUENCY

As we know, vibrational spectrum of a molecule or a cluster is intimately related with its intrinsic structure. We, therefore, compute the vibrational frequencies of all concerned diamondoids with the treatment of Gaussian 98 at the level of B3LYP. Tables II–XI list the calculated values and the assignments of the vibrational frequencies for the lowest-energy isomers in the considered polymantane-order clusters only. Overall, we could not find any imaginary frequency from our calculated frequencies, implying that all of the calculated isomers are stable or metastable.

We typically plot the vibrational density of states (VDOS) of four low-energy isomers as displayed in Fig. 8. It is observed that the vibrational frequencies of the diamondoids

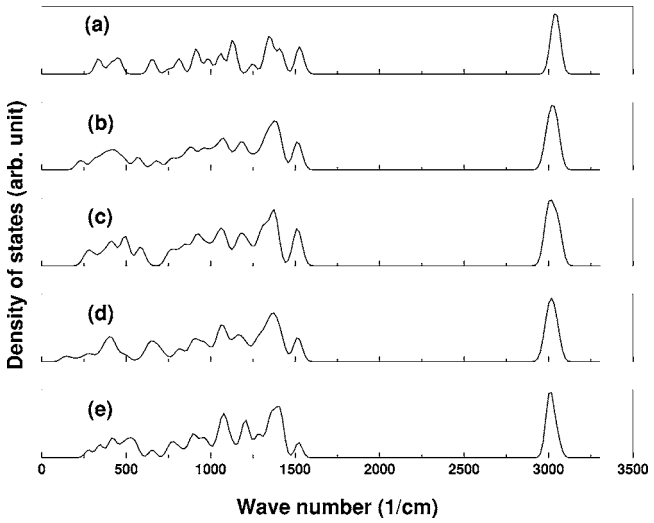

FIG. 8. The vibrational density of states (a)–(e) for the diamondoid(1), diamondoid(4), diamondoid(10), diamondoid(20), and diamondoid(27), respectively.

range from $\sim 150\ cm^{-1}$ to $\sim 3100\ cm^{-1}$. Clearly, each calculated VDOS consists of two bands: low-frequency bands ranging from $\sim 150\ cm^{-1}$ to $\sim 1600\ cm^{-1}$ and high-frequency bands ranging from $\sim 2900\ cm^{-1}$ to $\sim 3100\ cm^{-1}$. Between the two bands there manifests a big band gap. Analyzing the modes of the vibrational frequencies in detail, we found that the bands peaking at around $3040\ cm^{-1}$ are originated from the vibrations of H atoms in the diamondoids. These vibrational modes mainly characterize the C-H bonds stretched like those in the hydrogenated diamond (111) and (100) surfaces.[22,23] Structurally, there are different local configurations around each hydrogenated carbon atom, such as CH, CH_2, and CH_3, existing in many diamondoids, and thus the proximate environment of the H atoms in the diamondoids is not uniform. As suggested by Davidson and Pickett, [22] the bend modes of the neighboring CH_n ($n=1$, 2, and 3) may interact with each other. Thus, unlike the H stretch modes, the bend modes of C-H bonds are delocalized. Our calculations indicate that the bending modes of CH_n ($n=1$, 2, and 3) together with vibrational modes of all carbon atoms in a diamondoid make their contributions of the vibrational frequencies to the low-frequency bands in the VDOS.

In order to study the evolution of local vibrational properties against different atomic shell with respect to the mass center for a diamondoid, we calculate the local vibrational density of states (LVDOS) through projecting the VDOS onto each atomic shell for decamantane, as shown in Fig. 9. Strikingly, the high-frequency band together with the peak at around $1500\ cm^{-1}$ is resulted from H atoms; the LVDOS of inner carbon atoms in the decamantane is somewhat similar with that of bulk diamond. With the location of a carbon atom approaching the surface of the diamondoid, the trend of LVDOS becomes different from that of carbon diamond. When the size of a diamondoid is too small to have inner carbon atoms in it, just like the adamantane, the VDOS as well as the LVDOS of such a diamondoid are distinct from

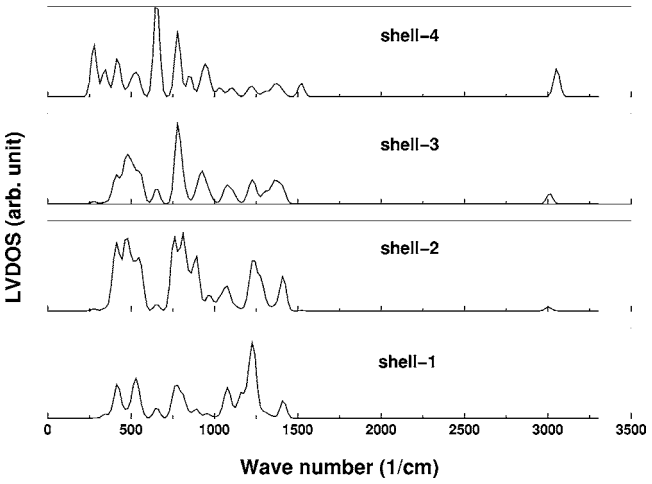

FIG. 9. The local vibrational density of states for the different atomic shells with respect to the mass center of a diamondoid(27). Shell-1 marked in the figure is to label the inner atomic shell and shell-4 to the outermost atomic shell.

the basic feature exhibited in the vibrational properties of bulk diamond at all. Overall, the higher diamondoids take the advantage of keeping the local vibrational properties of bulk diamond partly.

VIII. CONCLUSION

We systematically study the electronic and vibrational properties of diamondoid hydrocarbons based on ab initio calculations, and find that as the polymantane size of the diamondoid decreases, the diamondoid becomes more stable energetically, while its IP's and AE's as well as hardness increase. Through calculating the dissociation energies of possible fragmentation channels, we not only propose the lowest energy dissociation pathways for the considered cationic and neutral diamondoids, but also reveal that the products of the diamondoid dissociation preferably contain tiny hydrocarbons. Moreover, the vibrational frequencies of the diamondoids are predicted, which could be an indicator in identifying the different diamondoids in experiment. In addition, the detailed analysis of the vibrational density of states reveals that the two sharp peaks at about 3040 cm^{-1} and 1500 cm^{-1} are associated with the stretch modes and bend modes of H atoms, respectively. The inner carbon atoms in higher diamondoids may exhibit the local vibrational property of bulk diamond in part.

ACKNOWLEDGMENTS

This work is supported by the Fund of University of Science and Technology of China, the Fund of Chinese Academy of Science, and Grant No. NSFC50121202.

*Corresponding author. Electronic address: bcpan@ustc.edu.cn

[1] Landa. S. Machecek, and V. Mzourek, Collect. Czech. Chem. Commun. **5**, 1 (1933).
[2] J. E. Dahl, J. M. Moldowan, K. E. Peters, G. E. Claypool, M. A. Rooney, G. E. Michael, M. R. Mello, and M. L. Kohnen, Nature (London) **399**, 54 (1999).
[3] Linda K. Schulz, Arnd Wilhelms, Elin Rein, and Arne S. Steen, Org. Geochem. **32**, 365 (2001).
[4] M. Schoell and Robert M. K. Carlson, Nature (London) **399**, 15 (1999).
[5] M. A. Mckervey, Tetrahedron **36**, 971 (1980).
[6] W. Burns, T. R. B. Mitchell, M. A. Mckervey, J. J. Rooney, G. Ferguson, and P. Roberts, J. Chem. Soc., Chem. Commun., **1976**, 893 (1976).
[7] J. E. Dahl, S. G. Liu, and R. M. K. Carlson, Science **299**, 96 (2003).
[8] M. A. Meador, Annu. Rev. Mater. Sci. **28**, 599 (1998).
[9] Y. Lifshitz, T. Kohler, T. Frauenheim, I. Guzmann, A. Hoffman, R. Q. Zhang, X. T. Zhou, and S. T. Lee, Science **297**, 1531 (2002).
[10] A. P. Marchand, Aldrichimica Acta **28**, 95 (1995).
[11] J. Reister, E. McGregor, J. Jones, R. Enick, and G. Holder, Fluid Phase Equilib. **117**, 160 (1996).
[12] Vicky S. Smith and Amyn S. Teja, J. Chem. Eng. Data **41**, 923 (1996).
[13] Gregory C. McIntosh, Mina Yoon, Savas Berber, and David Tomanek, Phys. Rev. B **70**, 045401 (2004).
[14] Jean-Yves Raty, Guilia Galli, C. Bostedt, Tony W. van Buuren, and Louis J. Terminello, Phys. Rev. Lett. **90**, 037401 (2003).
[15] M. J. Frisch *et al.*, GAUSSIAN 98, Revision A9 (Gaussian, Inc., Pittsburgh, PA, 1998).
[16] G. Herzberg, *Molecular Spectra and Molecular Structure, Electronic Spectra and Electronic structure of Polyatomic Molecules* (Van Nostrand, New York, 1966), Vol. III.
[17] G. Herzberg, *Molecular Spectra and Molecular Structure* (Krieger, New York, 1991), Vol.3.
[18] W. J. Hehre, L. Radom, P. von R. Schleyer, and J. A. Pople, *Ab Initio Molecular Orbital Theory* (Wiley, New York, 1986).
[19] We use the value E_C=−37.7760 hartree for energy of a single carbon atom and E_H=−0.5003 hartree for a single hydrogen atom to estimate the binding energies of diamondoid hydrocarbons.
[20] R. G. Parr and W. Yang, *Density Functional Theory of Atoms and Molecules* (Oxford University Press, New York, 1989).
[21] R. G. Parr and R. G. Pearson, J. Am. Chem. Soc. **105**, 7512 (1983).
[22] B. N. Davidson and W. E. Pickett, Phys. Rev. B **49**, 11253 (1994).
[23] S. Tong Lee and G. Apai, Phys. Rev. B **48**, 2684 (1993).